DOI: https://doi.org/10.57233/ijsgs.v12i3.1210 ISSNp: 2488-9229; ISSNe: 3027-1118

IJSGS FUGUSAU VOL. 12(3) WEBSITE: https://fugus-ijsgs.com.ng

INTERNATIONAL JOURNAL OF SCIENCE FOR GLOBAL SUSTAINABILITY

(A PUBLICATION OF FACULTY OF SCIENCE, FEDERAL UNIVERSITY GUSAU, NIGERIA)

Characterisation and Performance Evaluation of a Fishbone Biochar-Rice Husk Silica Nanoparticle Hybrid for the Removal of Micropollutants from Wastewater

Aminu Abdullahi Giyawa[1], Thompson Izuagie[2], Jamilu Usman[3], Mubarak Muhammad[4], and Bello Saadu[5].

[1]Department of Science Laboratory Technology, Umaru Ali Shinkafi Polytechnic, Sokoto, Nigeria.

[2]Department of Chemistry, National Open University of Nigeria, Abuja, Nigeria.

[3]Department of Chemistry, Sokoto State University, Nigeria.

[4]Department of Science Laboratory Technology, Umaru Ali Shinkafi Polytechnic, Sokoto, Nigeria.

[5]Department of Applied Chemistry, Umaru Ali Shinkafi Polytechnic, Sokoto, Nigeria.

Corresponding Author's E-mail: giyawaaminu@gmail.com

Received on: August, 2026 **Revised and Accepted on:** September, 2026 **Published on:** October, 2026

ABSTRACT

Wastewater contamination by toxic heavy metals, synthetic dyes, and pathogenic microorganisms poses significant environmental and public health risks. The conversion of agricultural and food-processing wastes into functional adsorbent materials offers a sustainable approach to wastewater treatment. This study investigated the physicochemical characteristics and pollutant removal performance of fishbone biochar (FBB), rice husk-derived silica nanoparticles (SiNPs), and an FBB-SiNPs hybrid prepared at a mass ratio of 2:1. Fishbone biochar was produced through pyrolysis, while silica nanoparticles were synthesised from rice husk ash and incorporated into FBB to produce the hybrid material. The prepared adsorbents were characterised using X-ray fluorescence (XRF), X-ray diffraction (XRD), Fourier-transform infrared spectroscopy (FTIR), scanning electron microscopy (SEM), and thermogravimetric analysis (TGA). Their treatment efficiencies were evaluated against five heavy metals (Pb, Cd, Cu, Zn, and Ni), methylene blue (MB) dye, and two bacterial species, Escherichia coli and Staphylococcus aureus. The results revealed that the hybrid exhibited the highest removal efficiencies for Cd^{2+} (98.3 ± 0.5%) and Cu^{2+} (97.7 ± 0.6%), whereas FBB reduced the residual concentrations of Pb^{2+}, Zn^{2+}, and Ni^{2+} to below the reported analytical detection limit of 0.001 mg/L. The hybrid also demonstrated the greatest reduction in MB absorbance at 662 nm, corresponding to an apparent removal efficiency of 95.45%. In the microbial assessments, SiNPs produced the highest reduction in the reported E. coli response (96.6%), whereas the hybrid achieved the highest reduction in the S. aureus response (94.4%). Overall, the findings demonstrated that pollutant removal performance depended on contaminant type, with hybridisation enhancing some treatment outcomes but not consistently outperforming the individual materials. Although the results highlight the potential of these waste-derived materials for multifunctional wastewater treatment, further investigations involving validated microbial enumeration, adsorption mechanisms, and real wastewater systems are required to establish their practical applicability.

Keywords: fishbone biochar, rice husk silica. hybrid adsorbent, heavy metals, wastewater treatment

1.0 INTRODUCTION

Wastewater contamination remains a significant environmental concern because effluents can contain toxic metals, synthetic dyes, suspended solids, organic chemicals, and microorganisms. Where treatment is inadequate, these contaminants may reach surface water and groundwater, damage aquatic ecosystems, and limit water suitability for domestic, agricultural, and industrial use. Because wastewater contains chemically diverse pollutants, a material that performs well against one contaminant may not perform equally well against others. Recent reviews describe adsorption and engineered sorbents as promising approaches, while emphasising that treatment performance depends on both material properties and operating conditions (Ahuja *et al.,* 2022) (Zhang *et al.,* 2025). In Nigeria, the need for locally appropriate treatment materials is especially relevant where monitoring and treatment infrastructure may be constrained. Regional studies cited in the original draft should be retained only after their bibliographic details and findings have been independently verified. Recent reviews describe biochar as a potentially low-cost adsorbent for diverse wastewater contaminants, while emphasising that its performance depends on feedstock and preparation conditions (Xiang *et al.,* 2020). Global assessments continue to identify safe water, sanitation, and wastewater management as essential components of sustainable development (UNESCO, 2024). Wastewater treatment may involve coagulation, precipitation, biological processes, membrane separation, and adsorption. Process selection depends on pollutant identity and concentration, wastewater chemistry, and available resources. Adsorption is widely investigated because surface chemistry, pore structure, and mineral phases can facilitate the retention of dissolved contaminants. Nevertheless, laboratory removal percentages should not be interpreted as evidence of full-

DOI: https://doi.org/10.57233/ijsgs.v12i3.1210 ISSNp: 2488-9229; ISSNe: 3027-1118
IJSGS FUGUSAU VOL. 12(3) WEBSITE: https://fugus-ijsgs.com.ng

scale effectiveness without validation under realistic water chemistry, hydraulic conditions, and regeneration cycles. Biochar is produced by thermochemical conversion of biomass under oxygen limited conditions; its properties depend on feedstock, pyrolysis temperature, heating rate, residence time, and post-treatment. Recent reviews report that these factors influence surface functional groups, porosity, and heavy metal interactions (Ahuja *et al.,* 2022) (Zhang et *al.,* 2025). The suitability of a treatment process depends on contaminant characteristics, treatment objectives, operational requirements, and the quality of the treated water (World Health Organization, 2022). Household access to safely managed drinking water and sanitation remains an ongoing global monitoring priority (World Health Organization & United Nations Children's Fund, 2023).

Fishbone waste can contain calcium and phosphorus rich mineral phases, including hydroxyapatite related compounds, while rice husk ash can serve as a silica precursor. Fishbone-derived hydroxyapatite has been investigated for heavy metal removal from aqueous systems (Hernández-Cocoletzi *et al.,* 2020), and recent work has further examined how calcination and pH affect metal adsorption by fishbone-derived hydroxyapatite (Moreno Carpinteyro *et al.,* 2026). Rice husk silica extraction and modification have also been reviewed as routes towards adsorbents for wastewater treatment (Ijaz *et al.,* 2025). These studies provide a rationale for evaluating the materials used here, but they do not establish the performance of the present samples; this must be determined from the experimental results. Rice husk derived silica and related silica-based materials have been investigated as value added products from agricultural residues for water treatment applications (Ijaz *et al.,* 2025). Combining biochar with silica may alter surface chemistry, pore accessibility, and the distribution of active sites. However, a composite does not necessarily outperform each component for every contaminant. The outcome depends on component ratio, dispersion, pore accessibility, solution conditions, and pollutant chemistry. Recent studies of modified biochars and carbon-based composites support the value of comparing the individual components with the resulting hybrid rather than presuming synergistic performance (Ahuja *et al.,* 2022) (Zhang *et al.,* 2025). The present study therefore compared FBB, SiNPs, and a hybrid prepared at a 2:1 biochar-to-silica mass ratio for five metals, MB, and two bacterial test organisms. The objective was to characterise the materials and evaluate their relative pollutant-removal performance under the experimental conditions used. Recent reviews also indicate that modified biochar and hybrid materials can provide complementary surface properties, although performance must be demonstrated experimentally for each contaminant system (Cheng *et al.,* 2021). Nitrogen doped and otherwise modified biochars have been reviewed as strategies for improving adsorption interactions with both inorganic and organic contaminants (Kasera *et al.,* 2022). Critical reviews of sewage sludge derived biochar also highlight the potential of waste derived carbonaceous materials while noting the need to evaluate contaminant specific performance and safe use of spent adsorbents (Rangabhashiyam *et al.,* 2022). The study thus aimed to prepare and characterise a hybrid material derived from fishbone biochar and rice husk silica nanoparticles and evaluate its effectiveness in removing heavy metals, methylene blue dye, and microbial contaminants from wastewater.

2.0 MATERIALS AND METHODS

2.1 Materials

Fishbone waste was collected from food vendors in Goronyo Local Government Area, Sokoto State, Nigeria, and used as the precursor for fishbone biochar (FBB). Rice husk was obtained from KK Technologies Ltd., Sokoto South Local Government Area, Sokoto State, Nigeria, and used as the precursor for rice husk derived silica nanoparticles (SiNPs). The prepared materials were designated fishbone biochar (FBB), rice husk derived silica nanoparticles (SiNPs), and the FBB-SiNPs hybrid.

The chemicals used in the preparation of the adsorbents included sodium hydroxide (NaOH), hydrochloric acid (HCl), and ethanol (C_2H_5OH). Sodium hydroxide was used for the alkaline extraction of silica from rice husk ash, while hydrochloric acid was used during silica preparation to adjust the pH. Ethanol was used as the dispersion medium during hybrid preparation. Distilled water was used for washing the raw materials and preparing aqueous solutions.

The treatment experiments involved aqueous solutions containing lead (Pb^{2+}), cadmium (Cd^{2+}), copper (Cu^{2+}), zinc (Zn^{2+}), and nickel (Ni^{2+}), as well as methylene blue ($C_{16}H_{18}ClN_3S$) dye. The microbial test organisms were *Escherichia coli* (*E. coli*) and *Staphylococcus aureus* (*S. aureus*). These materials and test organisms were used to evaluate the physicochemical characteristics and pollutant removal performance of FBB, SiNPs, and the FBB-SiNPs hybrid.

2.2. Preparation of fishbone biochar

Fishbone waste collected from food vendors in Goronyo Local Government Area, Sokoto State, Nigeria, was used as the precursor for fishbone biochar (FBB). The bones were air-dried for 48 h and then oven-dried at 105 °C for 24 h. The dried material was ground and sieved to obtain particles of approximately 0.2 mm. A 200 g portion of the prepared powder was pyrolysed at 600 °C for 3.5 h using a heating rate of 5 °C min^{-1}. The furnace was allowed to cool

DOI: https://doi.org/10.57233/ijsgs.v12i3.1210 ISSNp: 2488-9229; ISSNe: 3027-1118
IJSGS FUGUSAU VOL. 12(3) WEBSITE: https://fugus-ijsgs.com.ng

before the product was recovered. The resulting material was designated FBB. The atmosphere used during pyrolysis and the final recovered mass should be confirmed from laboratory records and reported because they affect reproducibility and yield.

A 200 g portion of the prepared fishbone powder was subjected to pyrolysis at 600 °C for 3.5 h using a heating rate of 5 °C min^{-1}. The furnace was allowed to cool before the resulting carbonaceous material was collected. The final product was designated fishbone biochar (FBB) and used as one of the adsorbents for subsequent characterisation and pollutant removal experiments.

2.3. Preparation of Rice Husk-Derived Silica Nanoparticles

Rice husk obtained from KK Technologies Ltd., Sokoto South Local Government Area, Sokoto State, Nigeria, was used to prepare silica. A 600 g portion of rice husk was heated at 700 °C for 4 h to produce rice husk ash. Subsequently, 50 g of the ash was mixed with 500 mL of 0.5 M sodium hydroxide (NaOH). The suspension was heated at 90 °C and stirred at 200 rpm for 3.5 h. The mixture was filtered through Whatman No. 41 filter paper, and hydrochloric acid (HCl) was added to the filtrate until pH 7 was reached. The silica-containing material was stirred for 24 h and aged for 48 h. The product was designated rice husk-derived silica nanoparticles (SiNPs). The volume and concentration of HCl, washing procedure, drying temperature, and recovered silica mass should be added from the laboratory record; they cannot be inferred reliably from the current draft.

A 50 g portion of the rice husk ash was mixed with 500 mL of 0.5 M sodium hydroxide (NaOH) solution. The mixture was heated at 90 °C and stirred at 200 rpm for 3.5 h to facilitate the dissolution of silica into the alkaline solution. Following extraction, the mixture was filtered through Whatman No. 41 filter paper to separate the insoluble residues from the silica containing filtrate. Hydrochloric acid (HCl) was subsequently added to the filtrate to adjust the pH to 7. The resulting silica containing material was stirred for 24 h and allowed to age for 48 h. This process facilitated the formation and maturation of the silica-based product. The resulting material was designated rice husk derived silica nanoparticles (SiNPs) and used for subsequent characterisation and preparation of the hybrid adsorbent.

2.4. Preparation of the FBB-SiNPs Hybrid

The hybrid was prepared at a 2:1 FBB-to-SiNPs mass ratio by combining 50 g of FBB with 25 g of SiNPs. The solids were dispersed in 200 mL of ethanol and stirred for 1 h, followed by sonication for 45 min. The suspension was dried at 80 °C for 12 h and then heated at 300 °C for 2 h under nitrogen. The final material was designated the FBB-SiNPs hybrid. The total initial solid mass was 75 g.

2.5. Characterisation of the Prepared Materials

The prepared FBB, SiNPs, and hybrid were characterised using XRF, XRD, FTIR, SEM, and TGA. XRF was used to determine elemental composition; XRD to identify crystalline phases; FTIR to examine characteristic vibrational bands; SEM to assess surface morphology; and TGA to evaluate thermal behaviour.

2.6. Heavy Metal Removal Experiments

The heavy-metal removal experiments were conducted to evaluate the performance of FBB, SiNPs, and the FBB-SiNPs hybrid in reducing the concentrations of lead (Pb), cadmium (Cd), copper (Cu), zinc (Zn), and nickel (Ni) in aqueous solutions. The experiments were performed to compare the pollutant removal performance of the individual adsorbents with that of the hybrid material.

For each metal-removal test, 3.0 g of the relevant adsorbent was contacted with 30 mL of the aqueous solution containing the target metal. FBB, SiNPs, and the hybrid were tested separately. Initial and residual metal concentrations were determined using atomic absorption spectrophotometry (AAS).

2.7. Methylene Blue Treatment

Methylene blue (MB) treatment was evaluated by UV-visible spectrophotometry. The initial solution absorbance was 0.967 at 662 nm. After treatment, the reported absorbance values were 0.083 for FBB, 0.056 for SiNPs, and 0.044 for the hybrid.

2.8. Microbial Response Assessment

The microbial response was assessed using Escherichia coli and Staphylococcus aureus, representing Gram-negative and Gram-positive bacteria, respectively. The manuscript reports percentage reductions at an adsorbent dose of 125 mg: 93.4%, 96.6%, and 95.4% for E. coli treated with FBB, SiNPs, and the hybrid, respectively; and 72.7%, 86.0%, and 94.4% for *S. aureus*.

In Nigeria, the need for locally appropriate treatment materials is especially relevant where monitoring and treatment infrastructure may be constrained. Studies have documented heavy metal concerns in water sources near mechanic workshops in Sokoto and groundwater quality influences associated with mining and agricultural activities in southeastern Nigeria (Isah *et al.,* 2012) (Itumoh *et al.,* 2015). Recent work also highlights locally derived materials and multifunctional treatment approaches as relevant directions for sustainable water purification in sub-Saharan Africa (Izuagie *et al.,* 2025) (Izuagie *et al.,* 2026). Fishbone-derived porous carbon/hydroxyapatite composites have also been discussed as a locally relevant option for wastewater treatment (Izuagie, 2026). The broader relevance of locally

DOI: https://doi.org/10.57233/ijsgs.v12i3.1210 ISSNp: 2488-9229; ISSNe: 3027-1118

derived multifunctional materials for water purification in sub-Saharan Africa has been reviewed recently (Izuagie *et al.,* 2026). Wastewater management is also recognised as an important component of infection prevention and antimicrobial-resistance control (World Health Organization *et al.,* 2020).

At an adsorbent dose of 125 mg, the reported reduction in *E. coli* was 93.40% for FBB, 96.60% for SiNPs, and 95.40% for the FBB-SiNPs hybrid. For *S. aureus*, the corresponding reported reductions were 72.70% for FBB, 86.00% for SiNPs, and 94.40% for the hybrid.

The results indicate that SiNPs produced the highest reported reduction in *E. coli*, whereas the FBB-SiNPs hybrid produced the highest reported reduction in *S. aureus*. These differences suggest that the relative performance of the materials depended on the bacterial species examined.

2.9 Statistical Analysis

Where applicable, measurements were reported as mean ± standard deviation (SD) from three replicates. Statistical comparisons were reportedly conducted using one-way analysis of variance (ANOVA) in SPSS (version 19). The significance threshold should be stated as $p < .05$, not $p > .05$.

3. RESULTS AND DISCUSSION

3.1. Characterisation of the Prepared Adsorbent Materials

The characterisation results demonstrated differences in the reported elemental composition and surface area properties of FBB, SiNPs, and the FBB-SiNPs hybrid. These properties provide a basis for interpreting the observed variation in treatment performance.

3.1.1 X-Ray Fluorescence (XRF) Analysis

Table 1: Elemental composition of FBB, SiNPs and FBB-SiNPs hybrid determined by XRF analysis

Components	Biochar	SiNPs	Hybrid
Si	0.7 ± 0.05	95.7 ± 0.10	13.1 ± 0.10
Al	0.1 ± 0.01	<0.01	<0.01
Ca	76.4 ± 0.20	0.9 ± 0.02	66.2 ± 0.30
K	0.2 ± 0.02	2.7 ± 0.05	0.2 ± 0.02
P	22.6 ± 0.10	0.7 ± 0.02	20.5 ± 0.10
Zn	0.10 ± 0.01	0.04 ± 0.01	0.10 ± 0.01

The XRF results presented in Table 1 revealed distinct elemental compositions for FBB, SiNPs, and the FBB-SiNPs hybrid. Fishbone biochar was predominantly composed of calcium (76.4 ± 0.20%) and phosphorus (22.6 ± 0.10%), with relatively small amounts of silicon (0.7 ± 0.05%), potassium (0.2 ± 0.02%), aluminium (0.1 ± 0.01%), and zinc (0.10 ± 0.01%). The predominance of calcium and phosphorus is consistent with the mineral-rich nature of fishbone-derived materials. However, XRF analysis alone cannot establish the specific crystalline phases present in the material. Therefore, any assignment of calcium-phosphate phases, including hydroxyapatite, should be supported by complementary X-ray diffraction (XRD) and Fourier-transform infrared (FTIR) analyses.

The SiNPs sample contained 95.7 ± 0.10% silicon, together with smaller proportions of potassium (2.7 ± 0.05%), calcium (0.9 ± 0.02%), phosphorus (0.7 ± 0.02%), and zinc (0.04 ± 0.01%). The high silicon content supports the successful production of a silicon-rich material from rice husk-derived feedstock. Similar investigations have demonstrated the preparation of silica nanoparticles from rice husk ash and the use of complementary characterisation techniques to examine their chemical composition and structural properties (Agusnar *et al.,* 2022; Dorairaj *et al.,* 2022). In particular, XRF provides information about elemental composition, whereas FTIR and XRD help establish the chemical bonding and structural characteristics of the resulting silica material. Nevertheless, the reported silicon percentage must be interpreted according to the instrument's reporting basis. If the results represent elemental silicon, they should not be described directly as the percentage purity of SiO_2 without appropriate conversion and confirmation.

The FBB-SiNPs hybrid contained 66.2 ± 0.30% calcium, 20.5 ± 0.10% phosphorus, and 13.1 ± 0.10% silicon, alongside smaller proportions of potassium and zinc. The coexistence of these principal elements is consistent with the presence of both the calcium- and phosphorus-rich FBB component and the silicon-rich SiNPs component in the hybrid material. However, elemental composition alone cannot establish the uniform distribution of silica throughout the biochar matrix, confirm interfacial bonding, or demonstrate the formation of a new chemical phase. Such interpretations require complementary evidence from scanning electron microscopy coupled with energy-dispersive X-ray spectroscopy (SEM-EDX), FTIR, and XRD.

The importance of combining these techniques is demonstrated in recent studies of rice husk-derived silica, in which elemental analysis, spectroscopy, diffraction, and microscopy were used together to establish the composition and structural properties of the synthesised materials (Agusnar *et al.,* 2022; Dorairaj *et al.,* 2022). Furthermore, the development of composite adsorbents containing different functional components provides an opportunity to investigate complementary material properties for water treatment. However, the effectiveness

DOI: https://doi.org/10.57233/ijsgs.v12i3.1210 ISSNp: 2488-9229; ISSNe: 3027-1118

of the present FBB-SiNPs hybrid for contaminant removal must be established from the adsorption and microbial-removal results rather than inferred from its XRF composition alone. Accordingly, the XRF findings provide a compositional basis for interpreting the subsequent characterisation and performance results.

3.1.2. FTIR analysis

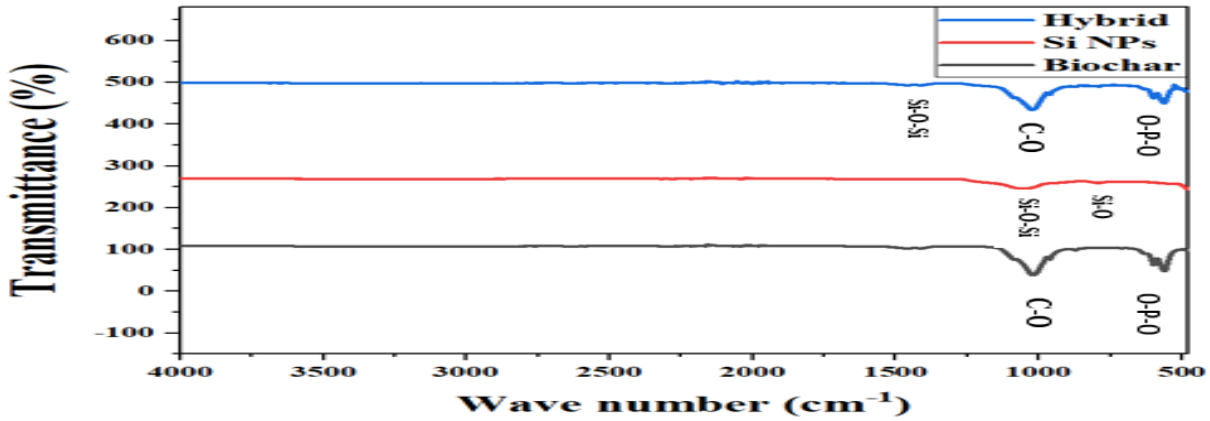


Figure 1: Fourier Transformed Infra-red Spectroscopy (FT-IR) Analysis

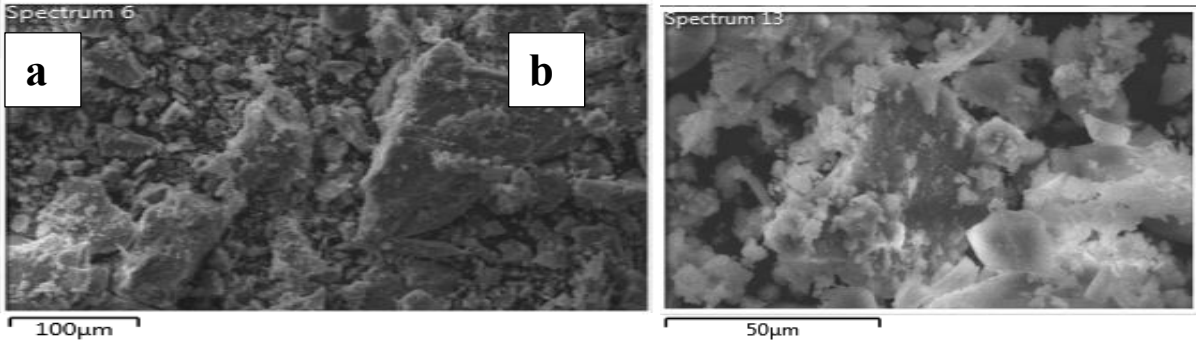
The FTIR spectrum of FBB showed bands within the reported 500-750 cm^{-1} region, which may be associated with phosphate-related vibrations in calcium-phosphate phases. Bands in the 1000-1200 cm^{-1} region may also arise from phosphate or other oxygen-containing groups; these assignments should be checked against the actual spectrum and peak positions. Functional groups can contribute to metal binding, but their role cannot be established from FTIR alone without complementary evidence.

The SiNP spectrum showed reported bands near 1080 and 400 cm^{-1}, which are broadly consistent with Si-O-Si stretching and bending vibrations, respectively. These bands support the formation of a silica-containing material. The term "silica nanoparticles" should be used consistently; the current data do not establish a nanotube morphology unless microscopy demonstrates tubular structures.

The hybrid spectrum contained bands attributed to both the FBB and silica components. This pattern is consistent with the coexistence of calcium-phosphate-containing and silica-containing phases in the prepared material.

3.1.3 Scanning Electron Microscopy (SEM)

The morphology of the prepared adsorbents is shown in Figure 2.



DOI: https://doi.org/10.57233/ijsgs.v12i3.1210 ISSNp: 2488-9229; ISSNe: 3027-1118

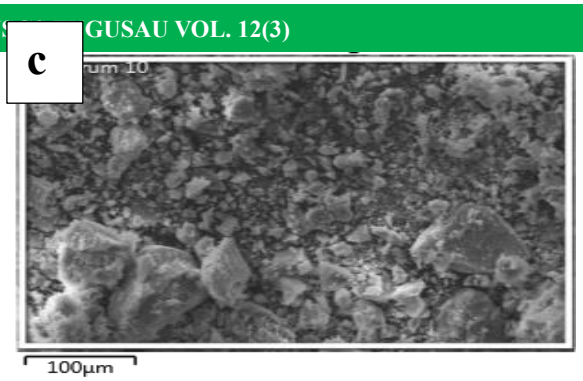


Figure 2: Scanning Electron Microscopy (a) Biochar (b) SiNPs (c) Hybrid

The FBB micrograph was described as showing a rough, irregular surface with cracks and cavities (Figure 2a). Such features may provide accessible sites for attachment or sorption, although SEM images alone do not quantify surface area or establish adsorption mechanisms. The SiNP sample appeared as aggregated particles (Figure 2b), a morphology that may reflect particle agglomeration. The hybrid image showed a heterogeneous surface consistent with the presence of both components (Figure 2c). Claims about pore blockage, nanoparticle anchoring, or improved accessible surface area should be made only where supported by the images and complementary surface-area measurements.

Overall, the SEM images suggest differences in surface morphology among FBB, SiNPs, and the hybrid. The images are qualitative evidence and should not be used alone to conclude that the hybrid has more adsorption sites or superior performance.

3.1.2 X-Ray Diffraction (XRD)

The XRD patterns of FBB, SiNPs, and the FBB-SiNPs hybrid are presented in Figure 3.

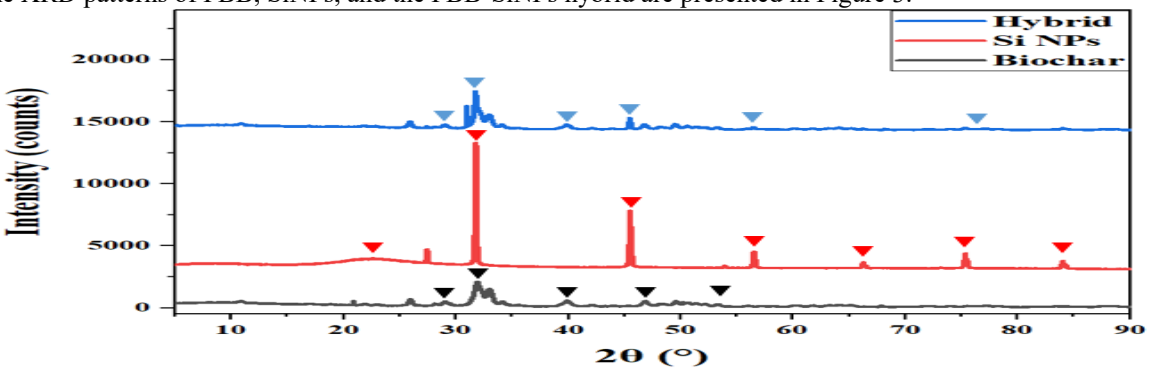


Figure 3: X-ray diffraction patterns of FBB, SiNPs and FBB-SiNPs

The XRD pattern of FBB displayed characteristic diffraction peaks associated with crystalline calcium-phosphate/hydroxyapatite phases. The observed reflections at approximately 2θ = 29.0°, 31.8°, 40.0°, 49.5°, and 53.0° are broadly consistent with crystalline mineral phases reported for fishbone-derived materials, although definitive phase identification requires comparison with reference diffraction data or a phase-matching analysis (Aryani & Riyadi, 2021; Moreno Carpinteyro *et al.,* 2026). The persistence of these reflections after pyrolysis suggests that the inorganic mineral component of the fishbone was retained during thermal conversion. Fishbone-derived hydroxyapatite has been identified as an important crystalline component in bone-based materials and investigated for heavy-metal adsorption (Moreno Carpinteyro *et al.,* 2026).

The SiNPs pattern was characterised mainly by a broad diffraction feature centred around approximately 2θ = 22°, which is commonly associated with predominantly amorphous silica. The broad feature suggests limited long-range crystalline order in the silica fraction. The interpretation of weaker reflections at higher diffraction angles should remain cautious because these features may arise from minor crystalline impurities or other phases and require confirmation against reference patterns (Ijaz *et al.,* 2025; Tessema *et al.,* 2023).

The XRD pattern of the FBB-SiNPs hybrid exhibited features attributable to both components. The persistence of fishbone-derived crystalline reflections alongside the broad silica-associated feature suggests that the hybrid retained structural contributions from FBB and SiNPs. This interpretation is consistent with the elemental composition

DOI: https://doi.org/10.57233/ijsgs.v12i3.1210 ISSNp: 2488-9229; ISSNe: 3027-1118
IJSGS FUGUSAU VOL. 12(3) WEBSITE: https://fugus-ijsgs.com.ng

indicated by XRF; however, XRD and XRF alone do not establish uniform silica distribution or chemical bonding between the components. Such conclusions would require supporting microscopy or additional surface analysis (Moreno Carpinteyro *et al.,* 2026; Tessema *et al.,* 2023).

3.1.6 Thermogravimetric Analysis (TGA)

The TGA curves of FBB, SiNPs, and the FBB-SiNPs are presented in Figure 3.4.

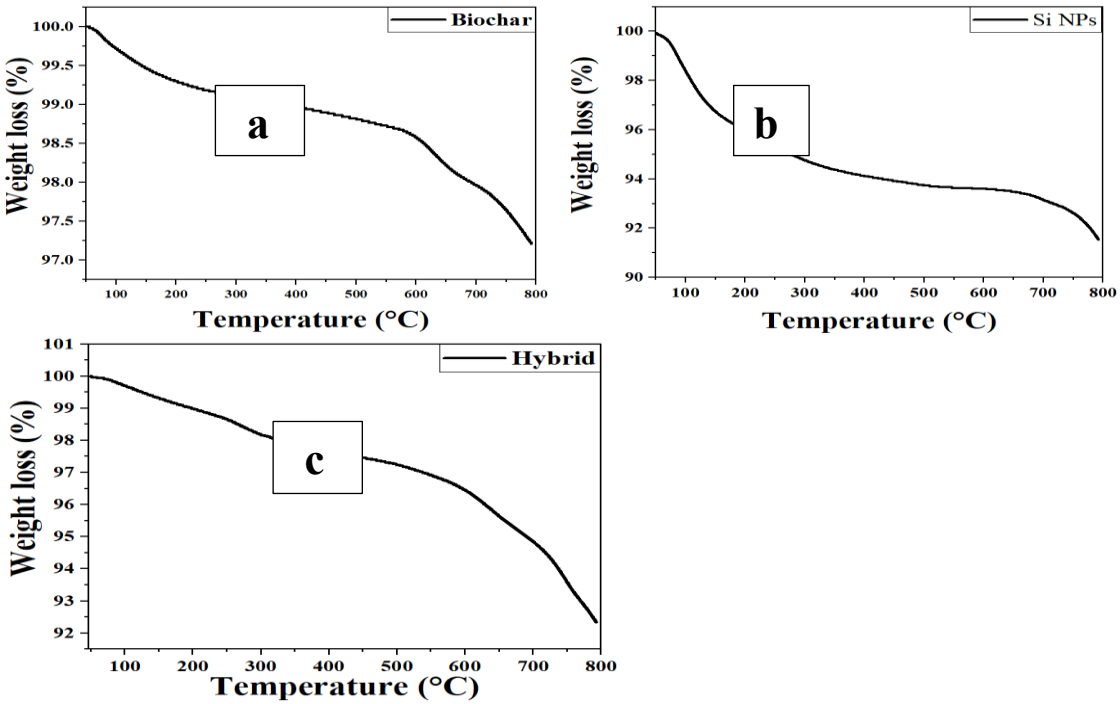


Figure 4: TGA curves of (a) FBB, (b) SiNPs and (c) FBB-SiNPs

The TGA profile of FBB showed relatively small mass loss over the investigated temperature range, with approximately 97% residual mass at 700 °C. This high residual mass is consistent with the substantial inorganic mineral fraction indicated by the XRF results. Calcium- and phosphorus-containing mineral phases can contribute to the residue remaining at elevated temperatures, as also observed in studies of fishbone-derived hydroxyapatite (Moreno Carpinteyro *et al.,* 2026). The TGA profile of SiNPs showed a gradual mass loss over the investigated temperature range, with approximately 91% residual mass at 800 °C. Mass loss at lower temperatures may be associated with the removal of adsorbed moisture, while further changes can reflect the behaviour of surface hydroxyl groups and residual impurities; these assignments depend on the test atmosphere and heating conditions (Tessema *et al.,* 2023). The hybrid showed approximately 92.5% residual mass at 800 °C. Its residual mass is consistent with a composite containing both mineral-rich FBB and silica-rich SiNPs, although the precise contributions of each component cannot be quantified from the reported curve alone. TGA is useful for comparing thermal mass-loss behaviour and residue, but thermal stability claims should be limited to the tested temperature range and atmosphere (Ravindiran et al., 2024; Yaashikaa *et al.,* 2020).

3.2. Heavy metal removal performance

3.2.1 Comparative Discussion of Heavy-Metal Removal

The results presented in Table 2 demonstrate that fishbone biochar (FBB), rice husk-derived silica nanoparticles (SiNPs), and the FBB–SiNPs hybrid exhibited high removal efficiencies for the five investigated heavy metals. The removal efficiencies varied according to the metal and adsorbent, indicating that the performance of the materials was metal-dependent. FBB recorded removal efficiencies greater than 99.9% for Pb^{2+}, Zn^{2+}, and Ni^{2+}, while the hybrid achieved the highest reported removal efficiencies for Cd^{2+} (98.3 ± 0.5%) and Cu^{2+} (97.7 ± 0.6%). These differences suggest that combining FBB with SiNPs modified the removal performance of the resulting material rather than uniformly improving its effectiveness for every metal. The metal-specific behaviour is consistent with the established influence of adsorbent composition, surface chemistry, and solution conditions on heavy-metal removal by biochar-based materials (Ahuja et al., 2022).

Table 2: Percentage removal of heavy metals by the prepared adsorbents

DOI: https://doi.org/10.57233/ijsgs.v12i3.1210 ISSNp: 2488-9229; ISSNe: 3027-1118

IJSGS FUGUSAU VOL. 12(3) WEBSITE: https://fugus-ijsgs.com.ng

Metal	FBB Removal (%)	SiNPs Removal (%)	Hybrid Removal (%)
Pb^{2+}	>99.9	87.6 ± 1.5	87.2 ± 1.8
Cd^{2+}	94.9 ± 1.2	96.0 ± 0.9	98.3 ± 0.5
Cu^{2+}	97.1 ± 0.8	96.7 ± 1.1	97.7 ± 0.6
Zn^{2+}	>99.9	>99.9	>99.9
Ni^{2+}	>99.9	98.6 ± 0.7	99.6 ± 0.3

For Pb^{2+}, FBB achieved removal greater than 99.9%, substantially exceeding the efficiencies recorded for SiNPs (87.6 ± 1.5%) and the hybrid (87.2 ± 1.8%). The superior performance of FBB may be associated with its calcium- and phosphorus-rich mineral composition, which could facilitate metal retention through ion exchange, surface interactions, and mineral precipitation. However, the specific contribution of these mechanisms cannot be established from removal efficiency and XRF results alone. The lower Pb^{2+} removal recorded for the hybrid suggests that incorporating silica did not enhance Pb^{2+} removal under the experimental conditions employed. This observation highlights the importance of evaluating composite adsorbents separately for individual contaminants rather than assuming that combining two materials will improve the removal of every metal.

For Cd^{2+}, the hybrid recorded the highest removal efficiency (98.3 ± 0.5%), compared with 96.0 ± 0.9% for SiNPs and 94.9 ± 1.2% for FBB. This result suggests that the combination of the calcium- and phosphorus-rich biochar fraction with the silica-containing component may have provided complementary surface properties favourable for Cd^{2+} retention. Possible contributing mechanisms include interactions with oxygen-containing surface groups, ion exchange, and precipitation involving mineral constituents. Nevertheless, additional experiments would be required to establish the relative importance of these mechanisms. The superior performance of the hybrid for Cd^{2+} indicates that its composition may be particularly favourable for removing this metal under the conditions investigated.

For Cu^{2+}, all three adsorbents exhibited high removal efficiencies, ranging from 96.7 ± 1.1% to 97.7 ± 0.6%. The hybrid achieved the highest removal (97.7 ± 0.6%), followed by FBB (97.1 ± 0.8%) and SiNPs (96.7 ± 1.1%). The relatively small differences indicate that all three materials were effective for Cu^{2+} removal under the experimental conditions. The slightly higher value recorded for the hybrid may reflect contributions from the mineral and silica-containing components. However, the overlapping variability means that these numerical differences should not automatically be interpreted as statistically significant without appropriate inferential analysis. Ahuja et al. (2022) similarly emphasised the importance of material modification and surface properties when evaluating the performance of biochar-based adsorbents for heavy-metal removal.

Zn^{2+} exhibited the highest reported removal efficiency across all three adsorbents, with FBB, SiNPs, and the hybrid each achieving greater than 99.9% removal. This result indicates that all three materials performed highly effectively for Zn^{2+} under the conditions investigated. Because the reported values exceed the analytical reporting threshold, the results should be presented as greater than 99.9% rather than as absolute 100% removal. The similar reported performance also means that no clear superiority among the three materials can be established for Zn^{2+} from these results alone. Further investigations involving different initial concentrations, solution pH values, and competing ions could help determine whether the observed performance is maintained under more complex water-treatment conditions.

For Ni^{2+}, FBB achieved removal greater than 99.9%, followed by the hybrid at 99.6 ± 0.3% and SiNPs at 98.6 ± 0.7%. The results indicate that FBB exhibited the highest reported Ni^{2+} removal, although the hybrid also demonstrated substantial effectiveness. The strong performance of FBB may be related to its mineral-rich composition and the potential interaction of Ni^{2+} with calcium-phosphate-containing phases. Incorporating SiNPs maintained a high removal efficiency but did not produce a higher reported value than FBB alone. This finding further demonstrates that the effect of hybridisation depends on the particular metal being treated.

Overall, the results demonstrate that the performance of the prepared adsorbents varied with the heavy metal. FBB was the best-performing material for Pb^{2+} and Ni^{2+}, while the hybrid achieved the highest reported removal efficiencies for Cd^{2+} and Cu^{2+}. All three adsorbents achieved greater than 99.9% removal of Zn^{2+}. These findings suggest that the hybrid offers potential advantages for selected metals but does not outperform its individual components across all contaminants. Consequently, the selection of an adsorbent for wastewater treatment should consider the target contaminant, the characteristics of the wastewater, and the reproducibility of the observed removal efficiencies. Further studies under different operating conditions would be useful for establishing the applicability of these materials to complex wastewater systems.

DOI: https://doi.org/10.57233/ijsgs.v12i3.1210 ISSNp: 2488-9229; ISSNe: 3027-1118

3.3. UV-Visible Analysis of Methylene Blue-Contaminated Water and Treated Filtrates

Figure 4 (renumbered to avoid duplication with the heavy-metal plot) compares the UV-visible spectra of untreated MB solution and filtrates obtained after treatment with SiNPs, FBB, and the hybrid. MB-I denotes the untreated solution; MB-S, MB-B, and MB-H denote the SiNP-, FBB-, and hybrid-treated filtrates, respectively. The absorbance values at 662 nm are summarised in Table 4.

The untreated MB solution had an absorbance of 0.967 at approximately 662 nm. This wavelength was used to track the characteristic visible absorption band of MB, which is commonly monitored by UV-visible spectrophotometry in adsorption studies. A reduction in absorbance after treatment indicates attenuation of the dye signal; quantitative concentration removal should be inferred only if the Beer-Lambert relationship was validated with an appropriate calibration curve and measurements remained within its linear range (Fernando *et al.,* 2021) (Onyango *et al.,* 2026). Methylene-blue adsorption is commonly monitored by measuring absorbance near the dye's visible absorption maximum, but concentration-based estimates require an appropriate calibration procedure (Mougnol & Rathilal, 2024).

Using the absorbance-based estimate, the residual absorbance of 0.056 for SiNPs corresponds to approximately 94.21% apparent removal. This estimate was calculated as $[(A_0 - A_e)/A_0] \times 100$, where A_0 is the initial absorbance and A_e is the absorbance after treatment. Similar absorbance-based monitoring is used in studies of dye adsorption, but the calculated value should not be described as a concentration-based removal efficiency unless calibration was performed (Fernando *et al.,* 2021) (Onyango *et al.,* 2026).

The FBB-treated solution had a residual absorbance of 0.083, corresponding to approximately 91.42% apparent removal. This result indicates a substantial decrease in the MB absorbance signal under the conditions used. Biochar-based materials have been investigated for dye remediation, with performance depending on feedstock properties, surface chemistry, and treatment conditions; however, the present data do not isolate the relative roles of pore filling, electrostatic interactions, or aromatic interactions (Fernando *et al.,* 2021) (Izuagie *et al.,* 2022a). The hybrid-treated solution had the lowest residual absorbance (0.044), corresponding to approximately 95.45% apparent removal. The absorbance-based ranking was hybrid (95.45%) > SiNPs (94.21%) > FBB (91.42%). The result suggests that the hybrid gave the strongest attenuation of the MB signal among the tested materials. This is consistent with the broader investigation of multifunctional and modified waste-derived materials for water purification (Izuagie *et al.,* 2022b) (Izuagie *et al.,* 2026). although replicate-level uncertainty and a validated calibration curve are needed to establish the robustness of the observed difference. Biochar-based dye adsorption has been demonstrated with several feedstocks, but the magnitude of removal varies with the material and operating conditions (Yu *et al.,* 2024). Recent work on biochar made from waste bamboo chopsticks also illustrates the continuing evaluation of waste-derived adsorbents for methylene-blue treatment (Nguyen *et al.,* 2024).

The hybrid's lower residual absorbance may reflect complementary surface properties of silica and biochar. Silica-containing surfaces and carbonaceous supports have been investigated in composite materials for water purification, including approaches that immobilise functional components on porous carbon supports (Izuagie *et al.,* 2022b). This remains a plausible explanation rather than a mechanism demonstrated by the present data; confirmation would require adsorption isotherms, pH-dependent tests, and post-treatment surface analysis. Recent studies continue to examine biochar and related functional adsorbents for methylene-blue removal from aqueous media (Kundu *et al.,* 2024). Magnetic biochar optimisation studies likewise show that preparation conditions can substantially affect dye-adsorption performance (Liu *et al.,* 2024).

DOI: https://doi.org/10.57233/ijsgs.v12i3.1210 ISSNp: 2488-9229; ISSNe: 3027-1118

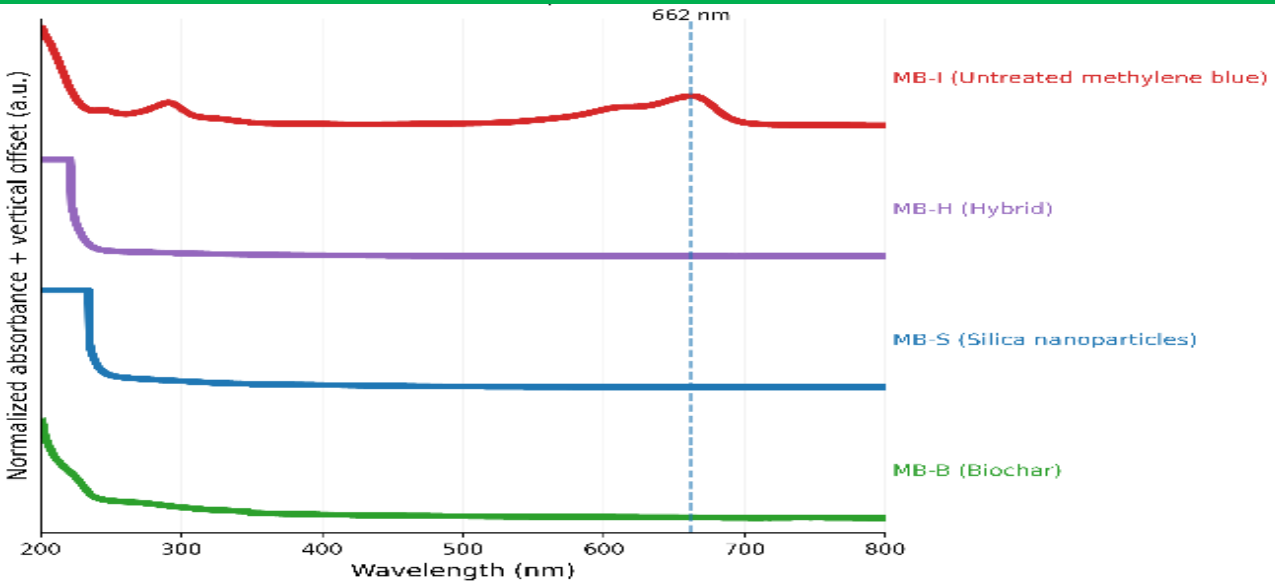


Figure 4: UV-visible spectra of untreated methylene-blue solution (MB-I) and filtrates treated with silica nanoparticles (MB-S), fishbone biochar (MB-B), and the FBB-SiNPs hybrid (MB-H). The untreated solution showed an absorption maximum at approximately 662 nm, while the signal was attenuated in the treated samples. If the spectra were normalised and vertically offset, this should be stated explicitly in the figure and the underlying unprocessed spectra should be retained.

Table 3. Quantitative comparison of methylene blue removal efficiency from contaminated water after filtration through silica nanoparticles, biochar, and the hybrid material.

Sample	Description	Absorbance at 662 nm, (Ae)	Apparent removal (%)
MB-I	Methylene blue-contaminated water	0.967	0.00
MB-S	Water filtrate through silica nanoparticles	~0.056	94.3
MB-B	Water filtrate through biochar	~0.083	91.42
MB-H	Water filtrate through hybrid material	~0.044	95.45

3.4 Removal of *E. coli*

The response of *E. coli* to FBB, SiNPs, and the hybrid was assessed at an adsorbent dose of 125 mg. The reported values are presented in Table 5. Before submission, the measurement endpoint must be clarified: the formula shown in the manuscript uses optical-density values, whereas the narrative refers to viable bacterial counts. Optical density does not directly quantify viable cells and cannot, by itself, demonstrate bacterial inactivation.

E. coli is a Gram-negative bacterium commonly used as an indicator of faecal contamination in water-quality assessment. The table reports control readings of 0.204 and 0.412, but the positive/negative control labels and their relationship to the percentage-reduction calculation require verification. The treated values were 0.027 for FBB, 0.014 for SiNPs, and 0.019 for the hybrid. These values and the reported reductions should be interpreted only after the measurement type and control definitions have been confirmed. Waste-derived porous carbon modified with copper nanoparticles has also been investigated for reducing microbial contaminants in polluted water (Izuagie *et al.,* 2022a).

Table 4. Reduction of *E. coli* by FBB, SiNPs and FBB-SiNPs at 125 mg

Treatment	Concentration	*E. Coli Value*	Inhibition Rate	(%) Reduction
+ Control–	0.204	–	–	
– Control	–	0.412	–	–
FBB	125 mg	0.027	0.385	93.4
SiNPs	125 mg	0.014	0.398	96.6
FBB-SiNPs	125 mg	0.019	0.393	95.4

The reported percentage response was calculated using the following expression, provided that OD values were the actual measured endpoint:

Percentage reduction (%) = $[(OD_i - OD_f) / OD_i] \times 100$

Where:

OD_i = optical density of the untreated control.

OD_f = optical density of the treated sample.

The reported reductions were 93.4% for FBB, 96.6% for SiNPs, and 95.4% for the hybrid. SiNPs therefore produced the largest reduction in the reported *E. coli* response at 125 mg, followed by the hybrid and FBB. Waste-derived porous carbon and modified carbon materials have previously been investigated for microbial contaminant treatment, including copper-nanoparticle-modified

DOI: https://doi.org/10.57233/ijsgs.v12i3.1210 ISSNp: 2488-9229; ISSNe: 3027-1118
IJSGS FUGUSAU VOL. 12(3) WEBSITE: https://fugus-ijsgs.com.ng

nanoporous carbon derived from eggshell waste (Izuagie *et al.,* 2022a). The comparison provides relevant context, but it does not independently validate the present measurements or establish that the observed response represents viable-cell inactivation. Reviews of biochar-based wastewater treatment identify biological contaminants as a relevant but methodologically distinct treatment target (Jagadeesh & Sundaram, 2023).

3.5. Removal of *S. aureus*

The response of *S. aureus* to FBB, SiNPs, and the hybrid was evaluated at an adsorbent dose of 125 mg. The control readings and treatment values are summarised in Table 6. As for *E. coli*, the endpoint must be confirmed because the draft alternates between optical-density measurements and viable counts. *S. aureus* is Gram-positive, but differences in cell-envelope structure alone cannot establish the mechanism responsible for the observed response.

Table 5. Reduction of *S. aureus* by FBB, SiNPs and FBB-SiNPs at 125 mg

Treatment | Dose |	Reported S. aureus value |	Reported response difference |	Reduction (%)
+ Control	—	0.212	—
— Control	—	0.392	—
FBB	125 mg	0.107	0.285	72.7
SiNPs	125 mg	0.055	0337	86.0
FBB-SiNPs	125 mg	0.022	0.370	94.4

The reported reduction in the *S. aureus* response was 72.7% for FBB, 86.0% for SiNPs, and 94.4% for the hybrid. The hybrid therefore produced the largest reduction in the reported endpoint at 125 mg. The pattern differs from the *E. coli* results, for which SiNPs gave the highest reported reduction. Studies of waste-derived nanoporous carbon modified with copper nanoparticles demonstrate that engineered carbon materials are being explored for microbial water treatment (Izuagie *et al.,* 2022a), while recent reviews emphasise the potential of multifunctional materials for complex contaminant removal (Izuagie *et al.,* 2026). These studies provide context rather than direct evidence for the mechanism or efficacy of the present FBB-SiNPs hybrid. Statistical significance cannot be claimed without verified replicate-level data and correctly reported inferential statistics. The use of carbonaceous supports carrying active components has also been reported for water purification, although the mechanism should not be inferred without direct testing in the present system (Izuagie *et al.,* 2022b).

Although the reported *S. aureus* response was reduced by 86.0% with SiNPs, the present results alone do not establish a specific antimicrobial mechanism. In particular, membrane disruption, oxidative stress, or a causal role for surface hydroxyl groups cannot be concluded without direct measurements. The interpretation is further limited because the manuscript alternates between optical-density readings and viable cell-counts. Optical density is not interchangeable with colony-forming units (CFU/mL), and confirmation by a validated culture-based method is needed before describing these values as bacterial inactivation or viable-cell removal. This distinction is important when assessing materials intended for multifunctional water purification (Izuagie *et al.,* 2026).

4.0 CONCLUSION

This study evaluated fishbone biochar (FBB), rice husk-derived silica nanoparticles (SiNPs), and their hybrid (2:1 mass ratio) for removing five heavy metals, methylene blue (MB), and two bacterial test organisms from aqueous solutions. Characterisation confirmed the calcium- and phosphorus-rich composition of FBB, the silicon-rich composition of SiNPs, and the presence of the principal elements from both materials in the hybrid. The hybrid achieved the highest reported removal of Cd (98.3 ± 0.5%) and Cu (97.7 ± 0.6%), while FBB reduced Pb, Zn, and Ni to below the stated detection limit. The hybrid also showed the highest apparent MB removal (95.45%). For microbial reduction, SiNPs performed best against *E. coli* (96.6%), whereas the hybrid achieved the highest reduction against *S. aureus* (94.4%).

Overall, the results demonstrated the potential of these materials for contaminant removal, although performance varied with the contaminant type. Further studies should validate the experimental conditions, assess adsorption mechanisms and kinetics, examine regeneration and leaching, and evaluate performance in real wastewater using appropriate statistical analyses and validated microbial enumeration methods. These investigations are necessary before practical application can be recommended.

5.0 REFERENCES

Agusnar, H., Sugita, P., & Nainggolan, I. (2022). Preparation sodium silicate from rice husk to synthesize silica nanoparticles by sol-gel method for adsorption water in analysis of methamphetamine. South African Journal of Chemical Engineering, 40, 80–86. https://doi.org/10.1016/j.sajce.2022.02.001

Ahuja, R., Kalia, A., Sikka, R., & Chaitra, P. (2022). Nano modifications of biochar to enhance heavy metal adsorption from wastewaters: A review. ACS Omega, 7(50), 45825–45836. https://doi.org/10.1021/acsomega.2c05117

Cheng, N., Wang, B., Wu, P., Lee, X., Xing, Y., Chen, M., & Gao, B. (2021). Adsorption of emerging contaminants from water and wastewater by modified biochar: A

review. Environmental Pollution, 273, Article 116448. https://doi.org/10.1016/j.envpol.2021.116448

Dorairaj, D., Govender, N., Zakaria, S., et al. (2022). Green synthesis and characterization of UKMRC-8 rice husk-derived mesoporous silica nanoparticle for agricultural application. Scientific Reports, 12, Article 20162. https://doi.org/10.1038/s41598-022-24484-z

Fernando, J. C., Peiris, C., Navarathna, C. M., Gunatilake, S. R., Welikala, U., Wanasinghe, S. T., Madduri, S. B., Jayasinghe, S., Mlsna, T. E., Hassan, E. B., & Ferez, F. (2021). Nitric acid surface pre-modification of novel Lasia spinosa biochar for enhanced methylene blue remediation. Groundwater for Sustainable Development, 14, Article 100603. https://doi.org/10.1016/j.gsd.2021.100603

Hernández-Cocoletzi, H., Salinas Domínguez, R. A., Águila-Almanza, E., Rubio-Rosas, E., Chai, W. S., Chew, K. W., Mariscal-Hernández, C., & Show, P. L. (2020). Natural hydroxyapatite from fishbone waste for the rapid adsorption of heavy metals of aqueous effluent. Environmental Technology & Innovation, 20, Article 101109. https://doi.org/10.1016/j.eti.2020.101109

Ijaz, S., Kausar, A., Iqbal, M., El Messaoudi, N., Miyah, Y., Knani, S., & Graba, B. (2025). Advances in extraction of silica from rice husk and its modification for friendly environmental wastewater treatment via adsorption technology. Journal of Water Process Engineering. https://doi.org/10.1016/j.jwpe.2025.107187

Isah, A., Uba, A., Izuagie, T., & Sadiq, S. I. (2012). Assessment of selected heavy metals in some water sources located close to mechanic workshop sites in Sokoto Metropolis. International Journal of Chemical Sciences, 5(1), 51–55.

Itumoh, E. J., Aghamelu, O. P., & Izuagie, T. (2015). Influence of mining and agricultural activities on the quality of groundwater from some rural areas of South-Eastern Nigeria. Global NEST Journal, 17(2), 406–417.

Izuagie, T. (2025). Harnessing locally derived biocomposites for sustainable water purification and environmental protection. In Proceedings of the 1st International Hybrid Conference of the Faculty of Science (IHCFS 2025) (pp. 270–286). Faculty of Science, Federal University Gusau. https://doi.org/10.57233/ihcfs.032

Izuagie, T. (2026). Fish-bone-derived porous carbon/hydroxyapatite composite for sustainable treatment of local sludge wastewater. In 11th Annual Symposium of ACS Nigeria: Book of Proceedings (pp. 22–29). American Chemical Society Nigeria International Chemical Sciences Chapter. https://acsnigeria.org/wp-content/uploads/2026/09/5-1.pdf

Izuagie, T., Muazu, S. A., & Anka, H. A. (2022a). Nanoporous carbon from waste egg shells modified with copper-nanoparticles: An efficient material for removal of microbial contaminants from polluted water. International Journal of Science for Global Sustainability, 8(4), 1–9. https://doi.org/10.57233/ijsgs.v8i4.360

Izuagie, T., Oyem, I. M., Umar, B., Isah, A., Abdulsalami, I. O., & Oyem, H. H. (2026). Sustainable water treatment in sub-Saharan Africa: Recent advances in multifunctional materials and digital tools for complex contaminant removal. Sustainability Science and Technology, 3(2), Article 022001. https://doi.org/10.1088/2977-3504/ae565e

Izuagie, T., Sirajo, M., & Abubakar, M. G. (2022b). Immobilization of polyoxometalate-ionic liquid on coconut shell nanoporous carbon support: An improved material for water purification. Caliphate Journal of Science and Technology, 4(2), 213–220. https://doi.org/10.4314/cajost.v4i2.11

Jagadeesh, N., & Sundaram, B. (2023). Adsorption of pollutants from wastewater by biochar: A review. Journal of Hazardous Materials Advances, 9, Article 100226. https://doi.org/10.1016/j.hazadv.2022.100226

Kasera, N., Kolar, P., & Hall, S. G. (2022). Nitrogen-doped biochars as adsorbents for mitigation of heavy metals and organics from water: A review. Biochar, 4, Article 17. https://doi.org/10.1007/s42773-022-00145-2

Kundu, D., Sharma, P., Bhattacharya, S., Gupta, K., Sengupta, S., & Shang, J. (2024). Study of methylene blue dye removal using biochar derived from leaf and stem of Lantana camara L. Carbon Research, 3, Article 22. https://doi.org/10.1007/s44246-024-00108-1

Liu, B., Wu, Y., Xing, Z., Zhang, J., & Xue, Y. (2024). Optimization of magnetic biochar preparation process, based on methylene blue adsorption. Molecules, 29(21), Article 5213. https://doi.org/10.3390/molecules29215213

Moreno Carpinteyro, M., Peñas Esteban, F. J., & Durán Benito, A. (2026). Fishbone-derived hydroxyapatite from distinct species: Effect of calcination and pH on heavy metal adsorption from water. Environments, 13(2), Article 102. https://doi.org/10.3390/environments13020102

Mougnol, J. B. B., & Rathilal, S. (2024). Functionalized bioadsorbent application on methylene blue removal from wastewater: A review. Advances in Materials Science and Engineering, 2024, Article 5704096. https://doi.org/10.1155/2024/5704096

Nguyen, T.-H., Hoang, H. T. T., & Vu, T. P. (2024). Ball-milled biochar from waste bamboo chopsticks: A potential adsorbent for methylene blue removal. Applied Environmental Research, 46(1). https://doi.org/10.35762/AER.2024004

Onyango, C., Nyairo, W., & Shikuku, V. (2026). A review on the recent advances in the use of hydrochar for adsorption of methylene blue dye from aqueous systems.

Discover Chemistry, 3, Article 20. https://doi.org/10.1007/s44371-026-00474-2

Rangabhashiyam, S., Lins, P. V. D. S., de Magalhães Oliveira, L. M. T., Sepulveda, P., Ighalo, J. O., Rajapaksha, A. U., & Meili, L. (2022). Sewage sludge-derived biochar for the adsorptive removal of wastewater pollutants: A critical review. Environmental Pollution, 293, Article 118581. https://doi.org/10.1016/j.envpol.2021.118581

Ravindiran, G., Rajamanickam, S., Janardhan, G., et al. (2024). Production and modifications of biochar to engineered materials and its application for environmental sustainability: A review. Biochar, 6, Article 62. https://doi.org/10.1007/s42773-024-00350-1

UNESCO. (2024). The United Nations world water development report 2024: Water for prosperity and peace. United Nations Educational, Scientific and Cultural Organization. https://www.unesco.org/reports/wwdr/2024/en

World Health Organization. (2022). Guidelines for drinking-water quality: Fourth edition incorporating the first and second addenda. World Health Organization.https://www.who.int/publications/i/item/9789240045064

World Health Organization, Food and Agriculture Organization of the United Nations, & World Organisation for Animal Health. (2020). Technical brief on water, sanitation, hygiene (WASH) and wastewater management to prevent infections and reduce the spread of antimicrobial resistance. World Health Organization. https://www.who.int/publications-detailredirect/9789240006416

World Health Organization, & United Nations Children's Fund. (2023). Progress on household drinking water, sanitation and hygiene 2000–2022: Special focus on gender. World Health Organization and UNICEF. https://washdata.org/reports/jmp-2023-wash-households

Xiang, W., Zhang, X., Chen, J., Zou, W., He, F., Hu, X., Tsang, D. C. W., Ok, Y. S., & Gao, B. (2020). Biochar technology in wastewater treatment: A critical review. Chemosphere, 252, Article 126539. https://doi.org/10.1016/j.chemosphere.2020.126539

Yaashikaa, P. R., Kumar, P. S., Varjani, S., & Saravanan, A. (2020). A critical review on the biochar production techniques, characterization, stability and applications for circular bioeconomy. Biotechnology Reports, 28, Article e00570. https://doi.org/10.1016/j.btre.2020.e00570

Yu, H., Zhang, Y., Wang, L., Tuo, Y., Yan, S., Ma, J., Zhang, X., Shen, Y., Guo, H., & Han, L. (2024). Experimental and DFT insights into the adsorption mechanism of methylene blue by alkali-modified corn straw biochar. RSC Advances, 14, 1854–1865. https://doi.org/10.1039/D3RA05964B

Zhang, K., Yi, Y., & Fang, Z. (2023). Remediation of cadmium or arsenic contaminated water and soil by modified biochar: A review. Chemosphere, 311, Article 136914. https://doi.org/10.1016/j.chemosphere.2022.136914

Zhang, X.-S., Chen, Y.-G., Wang, Q.-Y., & Sun, Y.-L. (2025). Advances in heavy metal wastewater treatment with biochar adsorption. Biofuels, Bioproducts and Biorefining, 19(6), 2399–2417. https://doi.org/10.1002/bbb.2751